ISSN 1063-7745, Crystallography Reports, 2015, Vol. 60, No. 4, pp. 525–531. © Pleiades Publishing, Inc., 2015.
Original Russian Text © V.V. Balaev, A.A. Lashkov, A.G. Gabdulkhakov, M.V. Dontsova, A.S. Mironov, C. Betzel, A.M. Mikhailov, 2015, published in Kristallografiya, 2015, Vol. 60, No. 4, pp. 579–585.

STRUCTURE OF MACROMOLECULAR COMPOUNDS

Three-Dimensional Structures of Unligated Uridine Phosphorylase from *Yersinia pseudotuberculosis* at 1.4 Å Resolution and Its Complex with an Antibacterial Drug

V. V. Balaev[a], A. A. Lashkov[a], A. G. Gabdulkhakov[a], M. V. Dontsova[a], A. S. Mironov[b], C. Betzel[c], and A. M. Mikhailov[a]

[a] *Shubnikov Institute of Crystallography, Russian Academy of Sciences, Leninskii pr. 59, Moscow, 119333 Russia*
[b] *State Research Institute of Genetics and Selection of Industrial Microorganisms, Pervyi Dorozhnyi proezd 1, Moscow, 117545 Russia*
[c] *University of Hamburg, Mittelweg 177, Hamburg, 20148 Germany*
e-mail: alashkov83@gmail.com

Received February 24, 2015

Abstract—Uridine phosphorylases play an essential role in the cellular metabolism of some antibacterial agents. Acute infectious diseases (bubonic plague, yersiniosis, pseudotuberculosis, etc., caused by bacteria of the genus *Yersinia*) are treated using both sulfanilamide medicines and antibiotics, including trimethoprim. The action of an antibiotic on a bacterial cell is determined primarily by the character of its interactions with cellular components, including those which are not targets (for example, with pyrimidine phosphorylases). This type of interaction should be taken into account in designing drugs. The three-dimensional structure of uridine phosphorylase from the bacterium *Yersinia pseudotuberculosis* (*Ypt*UPh) with the free active site was determined for the first time by X-ray crystallography and refined at 1.40 Å resolution (DPI = 0.062 Å; ID PDB: 4OF4). The structure of the complex of *Ypt*UPh with the bacteriostatic drug trimethoprim was studied by molecular docking and molecular dynamics methods. The trimethoprim molecule was shown to be buffered by the enzyme *Ypt*UPh, resulting in a decrease in the efficiency of the treatment of infectious diseases caused by bacteria of the genus *Yersinia* with trimethoprim.

DOI: 10.1134/S1063774515040069

INTRODUCTION

Pseudotuberculosis (Far East scarlet-like fever or scarlatinoid fever) is an acute infectious disease characterized by polymorphisms of clinical manifestations with the primary lesion of the gastrointestinal tract, the skin, and the musculoskeletal system [1, 2]. The causative agent of this disease—the bacterium *Yersinia pseudotuberculosis* (*Ypt*UPh)—belongs to the genus *Yersinia* of the family *Enterobacteriaceae* [2–4]. The bacteriostatic antibiotic trimethoprim (TOP) [PubChem CID 5578] is used in the treatment of diseases caused by bacteria of the genus *Yersinia* [5, 6]. Trimethoprim is an inhibitor of the bacterial enzyme dihydrofolate reductase essential for the survival of bacteria. It was shown [5, 6] that the bacteriostatic effect of this drug on bacteria of the genus *Yersinia* is associated with an increase in the activity of pyrimidine nucleoside phosphorylases.

Pyrimidine nucleoside phosphorylases are enzymes widespread in nature. They catalyze the reversible phosphorolysis of nucleosides to ribose 1'-phosphate (deoxyribose 1'-phosphate) and the corresponding pyrimidine base. Both thymidine phosphorylases and uridine phosphorylases from enterobacteriaceae were shown to possess thymidine phosphorylase activity [7]. Therefore, studies of uridine phosphorylases from different bacteria are not only of scientific interest, but also applied significance.

It was demonstrated [8] that *Ypt*UPh is an evolutionary precursor to the bacterium *Yersinia pestis* that causes the bubonic plague. Investigations of the structural aspect of interactions between antibacterial agents and uridine phosphorylase *Ypt*UPh are important from the standpoint of designing new drugs for the treatment of diseases caused by bacteria of the genus *Yersinia*. In the present work, we investigated the three-dimensional structure of uridine phosphorylase from *Ypt*UPh at high resolution (ID PDB: 4OF4; resolution 1.40 Å, DPI = 0.062 Å), found the binding site for the nucleoside antibiotic trimethoprim, and characterized interactions of this antibiotic with uridine phosphorylase from this bacterium.

Table 1. Data on the production of the enzyme *Yersinia pseudotuberculosis* uridine phosphorylase

Forward primer*	5'-GGGGAATTCGTTGGCGCGATTCATGCCTCGG-3'
Reverse primer*	5'-GCGGGATCCGGATTACAGCAGATGACGAGCGG-3'
Cloning vector	the pUC19 multi copy vector
Expression vector	the pUC19 multi copy vector
Producer organism	Escherichia coli
Amino-acid sequence of the final enzyme	MAKSDVFHLGLTKNDLQGATLAIVPGDPQRVEKIAK LMDNPVHLASHREFTSWRAELDGKAVIVCSTGIGGP STSIAVEELAQLGVRTFLRIGTTGAIQPHINVGDVLVT TAAVRLDGASLHFAPMEFPAVADFSCTTALVNAAKS VGATTHIGITASSDTFYPGQERYDTFSGRVVRHFKGS MEEWQSMGVMNYEMESATLLTMCASQGLRAGMV AGVIVNRTQQEIPNEETMKATESHAVKIVVEAARHL L

* The underlined symbols indicate the nucleotide sequence recognized by restriction enzymes.

MATERIALS AND METHODS

Cloning of the Uridine Phosphorylase Gene YptUPh

The cloning and expression of the uridine phosphorylase gene, as well as the isolation and purification of this enzyme from *Ypt*UPh, were described for the first time in sufficient detail in [7, 9]. Certain details concerning these procedures are summarized in Table 1.

Isolation and Purification of the Protein Uridine Phosphorylase YptUPh

The AM2009 strain containing the plasmid pMZ18 was grown in a complete Luria broth medium supplemented with ampicillin (100 μg/mL) in 1-L flasks for 16 h at 37°C with shaking (250 rpm). The cells were precipitated by centrifugation. The yield of the biomass was ~5 g/L. The cells were resuspended in a 50 mM Tris-HCl buffer, pH 7.5, containing 5 mM β-mercaptoethanol and 0.3 mM phenylmethylsulfonyl fluoride (phenyl methane sulfonyl fluoride, PMSF) and disintegrated by ultrasound. After centrifugation, a 10% (v/v) polyethyleneimine (Polymin P) solution (pH 6.0) was added to the supernatant, and the mixture was incubated with stirring for 12 h at 30°C. The precipitate was resuspended in a 50 mM Tris-HCl buffer, pH 7.5, containing 2 M ammonium sulfate, 5 mM β-mercaptoethanol, and 0.3 mM PMSF and then incubated for 12 h at 30°C.

Then the precipitate was concentrated by centrifugation at low speed, resuspended in a 50 mM Tris-HCl buffer, pH 7.5, containing 2 M ammonium sulfate, and separated on butyl-Sepharose columns (Amersham Pharmacia Biotech) equilibrated with the same buffer. The protein was eluted using an ammonium sulfate gradient (from 2 to 0 M) at a flow rate of 0.5 mL/min. The collected fractions were analyzed by sodium dodecyl sulfate polyacrylamide gel electrophoresis (SDS–PAGE) under denaturing conditions.

In the second step of the purification, the collected fractions of *Ypt*UPh were dialyzed against a 50-mM Tris-HCl buffer, pH 7.5, containing 20 mM NaCl and then applied to Q-Sepharose columns equilibrated with the same buffer. The protein was eluted using a NaCl gradient (from 20 mM to 1 M) at a flow rate of 1 mL/min. The collected fractions were subjected to SDS–PAGE under denaturing conditions; dialyzed against a 20 mM Tris-HCl buffer, pH 6.5, containing 20 mM NaCl; and concentrated to 15 mg/mL in the same buffer.

The homogeneity of the enzyme based on the results of 15% SDS-PAGE was not lower than 95%. The specific activity was 280 units/μL.

Crystallization of Unligated YptUPh

The screening of crystallization conditions for uridine phosphorylase from *Ypt*UPh was performed at 295 K by the sitting-drop vapor-diffusion technique using MbClass and MbClassII crystallization kits (Qiagen, Germany). The drops were composed of 5 μL of an *Ypt*UPh solution with a protein concentration of 10 mg/mL and 5 μL of the reservoir solution. The volume of the reservoir solution was 500 μL. The best initial conditions were optimized by varying the pH value of the buffer and the amount of the precipitant. Crystals with dimensions of 200 × 50 × 50 μm were obtained in one week. The crystallization conditions and the characteristics of the solutions are given in Table 2.

Structure Solution and Refinement

The experimental X-ray diffraction intensities were collected from a crystal of unligated *Ypt*UPh at 100 K at the P11 MX1, PETRA III facility for structural biology (DESY, Hamburg, Germany). Before exposure to X-rays, the crystal was soaked in a cryoprotectant solution composed of the reservoir solution supplemented with 40% (v/v) PEG 400.

Table 2. Crystallization of *Yersinia pseudotuberculosis* uridine phosphorylase

Method	Sitting-drop vapor-diffusion
Crystallization temperature, K	277
Protein concentration	15 mg/mL
Composition of the protein solution	20 mM Tris-HCl buffer, pH 6.5, 20 mM NaCl
Composition of the reservoir solution	1 *M* Tris, 5% (w/v) polyglutamic acid, 20% (w/v) PEG 2000, pH 7.8
Drop volume ratio	5 μL of protein and 5 μL of reservoir solution
Volume of the reservoir solution	500 μL

Table 3. X-ray-data collection and processing statistics for *Yersinia pseudotuberculosis* uridine phosphorylase

Sp. gr.	*H*3
a, *b*, *c*, Å	150.95, 150.95, 46.23
α, β, γ, deg	90, 90, 120
T, K	100
λ, Å	1.000
Crystal-to-detector distance, mm	236.7
Scan step, deg	0.2
Scan range, deg	180
Exposure time, s	1
Mosaicity, deg	0.15
Resolution range, Å	75.475–1.4000 (1.480–1.400)*
Total number of reflections	378866 (53029)*
Number of unique reflections	76922 (11096)*
Completeness, %	99.800 (99.000)*
Redundancy	4.900 (4.800)*
Average $I/\sigma(I)$	14.7 (1.20)*
Radiation source	PETRA III, (DESY, Hamburg, Germany)
Detector	PSI Pilatus 6*M*

*Data for the last high-resolution shell are given in parentheses.

The X-ray diffraction data were processed using the XDS [10] and Scala [11] programs and the CCP4 suite [12]. Crystallographic parameters and the X-ray data-collection statistics are given in Table 3.

The initial phases of the structure factors for *Ypt*UPh were obtained by the molecular-replacement method using the Phaser program [13] included in the CCP4 suite. The structure solution was searched for in the resolution range from 43.60 to 2.40 Å. The best solution of the model is characterized by Z-score = 44.4, R_{factor} = 26.7%; the correlation coefficient was 49.9%. One homodimer was located per asymmetric unit.

Table 4. Structure solution and refinement of *Yersinia pseudotuberculosis* uridine phosphorylase

Resolution range, Å	75.4700–1.4000 (1.4380–1.4020)*
Completeness, %	99.9
Number of reflections in the working set	76922 (5318)*
Number of reflections in the test set	3859 (277)*
R_{work}	0.152 (0.254)*
R_{free}	0.184 (0.279)*
Cruickshank DPI	0.0794
Number of refined non-hydrogen atoms:	
of protein	3770
of ions	1
of ligands	19
of water	434
Total	4224
R.m.s.d. from ideal geometry:	
bond lengths, Å	0.007
bond angles, deg	1.165
Average *B* factor, Å^2:	
for protein atoms	17.6
for ions	14.8
for ligand	34.2
for water	29.6
Ramachandran statistics:	
Number of residues in the most favored region, %	98.3
Number of residues in the disallowed region, %	1.32

*Data for the last high-resolution shell are given in parentheses.

The three-dimensional structure was refined using the Phenix [14] and Refmac 5 [15] program packages. The R_{free} value was calculated using a set of 5% of |**F**| randomly set aside. The results of the structure refinement were visually inspected and the manual rebuilding of the structure was performed with the Coot interactive graphics program [16, 17]. The atoms of the enzyme and the ligands were located in σ_A-weighted Fourier maps calculated with the mFo-DFc and 2mFo-DFc coefficients. In the final refinement cycles, the atomic displacement parameters for all atoms were refined in the anisotropic approximation. The validity of the refined structure was checked with the Coot [16, 17] and MolProbity [18] programs and using the PDB Validation Server (http://validate.rcsb.org/). The structure-refinement statistics are given in Table 4.

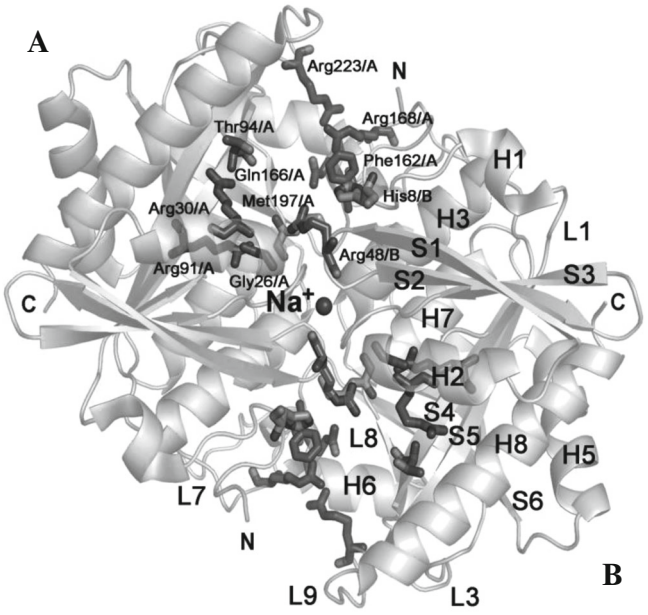

Fig. 1. Three-dimensional structure of the homodimer of *Ypt*UPh. The active-site residues of both subunits are shown. The secondary-structure elements are labeled. The figure is drawn with the PyMol program [28].

Computer Simulation

In order to locate the trimethoprim molecule in the active site of the homodimer of uridine phosphorylase *Ypt*UPh, molecular simulation was performed using the extra precision (XP) algorithm of the Glide program [19, 20] implemented in the Schrodinger suite (https://www.schrodinger.com). The position of the ligand was modeled and interactions of the ligand with atoms of amino-acid residues of the target enzyme were calculated in a cubic box with a 12-Å edge length. The position of the cubic box was specified based on the position of the binding-site residues of *Ypt*UPh. Several possible solutions were found, and the solution with the largest value of the GlideScore scoring function was selected. According to this solution, the ligand forms four hydrogen bonds. The molecular dynamics (MD) simulation of interactions of uridine phosphorylase with the ligand was carried out using the GROMACS program package [21] with a set of GROMOS all-atom force fields [22] and the 2-fs integration time step. Water molecules were described by the SPC216 three-point model. Electrostatic interactions were calculated using the particle-mesh Ewald (PME) technique [21]. The pressure in the system was maintained at 1 atm by applying the Berendsen barostat. The temperature of the MD system was kept constant at 300 K using the V-rescale thermostat. Van der Waals interactions were calculated with a smooth switching function in the range from 10 to 12 Å. The goal of the MD simulation was to check the stability of interactions between the active-site residues of *Ypt*UPh and trimethoprim. It was found that the trimethoprim molecule was bound to the enzyme during all 50-ns integrated trajectories.

RESULTS AND DISCUSSION

Structure of Uridine Phosphorylase from YptUPh

The quaternary structure of the *Ypt*UPh molecule is a hexamer composed of three homodimers. The arrangement of the monomers in the hexameric molecule of the enzyme is described by the point-group symmetry $L_3 3 L_2$. The hexameric molecule is formed via hydrogen bonds and hydrophobic interactions both between the residues of adjacent homodimers and within the central channel between the subunits related by a threefold axis.

The main hydrogen bonds between two adjacent homodimers and between the subunits in the homodimer are similar to those between the subunits of bacterial uridine phosphorylases from *Salmonella typhimurium* (*St*UPh) [23, 24] and *Escherichia coli* (*Ec*UPh) [25] studied earlier.

According to the Rossmann classification [26], the three-dimensional structure of the subunit of *Ypt*UPh has a three-layer αβα-sandwich architecture. Te following residues in *Ypt*UPh, unlike *St*UPh and *Ec*UPh, form additional hydrogen bonds: Lys36, Asn40, His43, Ser135, and His251. Each of these hydrogen bonds was found to be an interaction between amino-acid residues within the secondary-structure elements and, consequently, contributes to the conformational stability of the tertiary structure of the subunit of uridine phosphorylase *Ypt*UPh when compared with *St*UPh and *Ec*UPh.

Spatial Organization of the Active Site in YptUPh

The residues involved in the active site of uridine phosphorylase were found in [9]. In each homodimer there are two active sites formed by amino-acid residues of both subunits (Fig. 1). The active site of the subunit *A* is composed mainly of the residues of this subunit and involves two residues of the subunit *B*. The active site of the subunit *B* is formed in a similar way.

Each active site includes the nucleoside- and phosphate-binding sites (NBS and PBS, respectively). The nucleoside-binding site in subunit *A* is formed by the residues Phe162/A, Gln166/A, Arg168/A, Arg223/A, Met197/A, Arg48/B, and His8/B. In turn, NBS is divided into the following subsites: the uracil-binding site (residues Phe162/A, Gln166/A, Arg168/A, and Arg223/A) and the ribose-binding site (Met197/A, His8/B, and Arg48/B). The phosphate-binding site is composed of residues Gly26/A, Arg30/A, Arg48/B, Arg91/A, and Thr94/A.

In [25] it was noted for the first time that, depending on the presence or absence of the substrate in the active site of *Ec*UPh, one of the secondary-structure elements—loop L9—can exist in three different conformations corresponding to the open, intermediate,

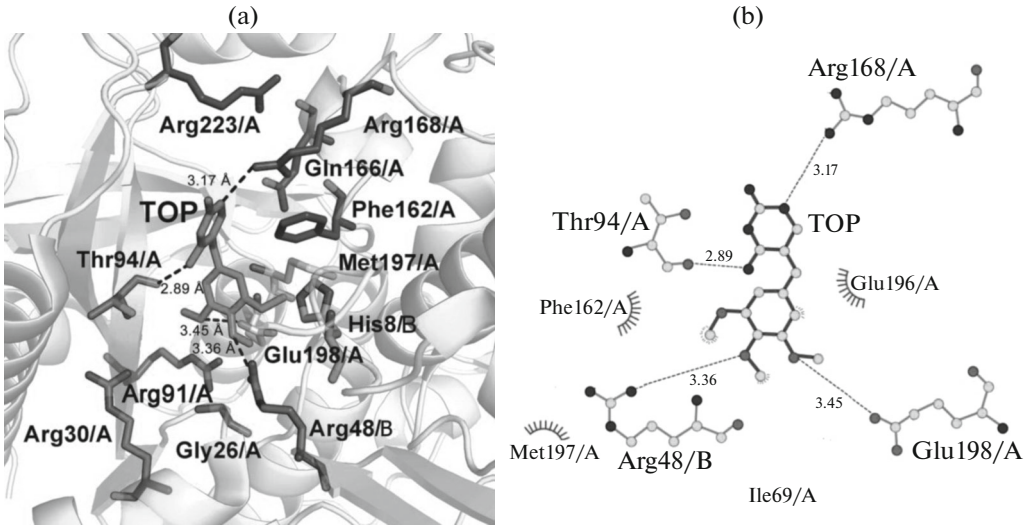

Fig. 2. (a) Three-dimensional organization of the active site in the complex of *Ypt*UPh with trimethoprim (TOP). (b) The schematic representation of interactions between TOP and the residues of the binding pocket of the enzyme *Ypt*UPh.

or closed conformation of the active site; i.e., the position of loop L9 (residues 223–230) has a considerable effect on the state of the active site in uridine phosphorylase. The differences in the position of loop L9 in the structures of bacterial uridine phosphorylases from different sources are no larger than this difference between the subunits of one homodimer in the structure of uridine phosphorylase from one source.

Binding of the Antibacterial Drug Trimethoprim

In order to study the structural aspects of interactions between the antibacterial drug trimethoprim (ID PDB:1DYR) and *Ypt*UPh, we performed molecular simulation. It was found that the trimethoprim molecule is located in the binding-site region of the enzyme (Fig. 2a). Trimethoprim binds to the residues involved in the uracil- and ribose-binding sites. In addition, the ligand is bound via hydrophobic interactions with the residues Ile69/A, Arg91/A, Ile92/A, Gly93/A, Glu196/A, Met215/A, and Ile220/A (Fig. 2b).

The trimethoxybenzene moiety of trimethoprim is located in the uracil-binding-site region (Fig. 2a). This moiety is composed of a hydrophobic aromatic ring with oxygen atoms serving as hydrogen-bond acceptors. The ribose in the native substrate (uridine) contains oxygen atoms, which can serve both as hydrogen-bond donors and acceptors. The pyrimidine-2,4-diamine moiety of trimethoprim located in the uracil-binding-site region is composed of a pyrimidine ring with two amino groups in positions 4 and 6. The nitrogen atoms of the amino groups can serve both as hydrogen-bond donors and acceptors. The uracil moiety contains carbonyl groups in these positions, and their oxygen atoms can serve only as hydrogen-bond donors. Although there is a certain similarity between trimethoprim and the native substrate, the type of inhibitors to which TOP can be assigned is an open question. It is known that 2,2'-anhydrouridine (ANU) studied earlier [27] is a high-affinity competitive inhibitor of bacterial uridine phosphorylases. To serve as a competitive inhibitor, the latter should contain groups similar to those in the natural substrate, whereas groups necessary for the reaction to occur should be absent. Trimethoprim substantially differs from ANU, but the number of hydrogen bonds formed with the enzyme differs only by one (Fig. 3). The hydrogen-bond lengths in the complex *St*UPh + ANU

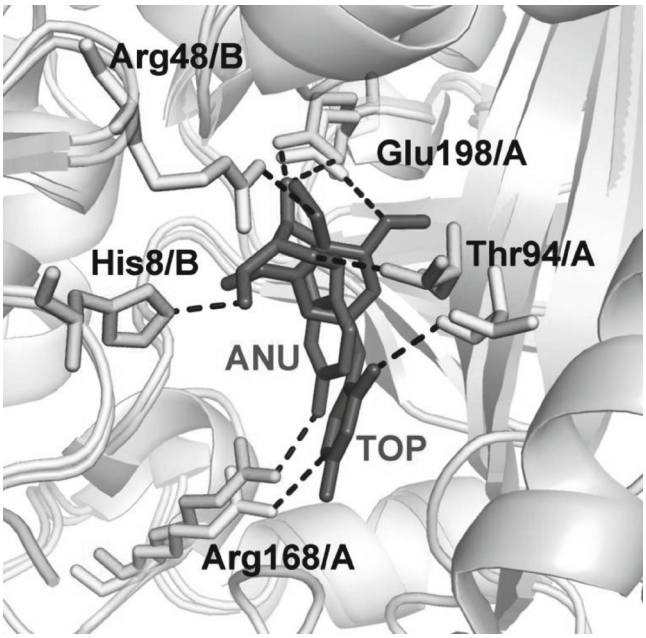

Fig. 3. Superposition of the three-dimensional structures of the active sites of *Ypt*UPh in complexes with trimethoprim (TOP) and 2,2'-anhydrouridine (ANU) [27]. The figures are drawn with the PyMol program [28].

vary from 2.4 to 3.4 Å; in the complex *Ypt*UPh + TOP, they vary from 2.9 to 3.5 Å.

The antibiotic cannot undergo degradation. First, uridine phosphorylase catalyzes the cleavage of nucleosides at the N1-glycosidic bond between the nitrogenous base and the ribose component of the ligand. In trimethoprim this covalent bond is absent. Second, the nature of functional chemical groups of the bacteriostatic drug interacting with *Ypt*UPh differs from that of the functional groups of the substrates of this enzyme. Thus, TOP contains the pyrimidine-2,4-diamine moiety instead of the uracil component of the substrate (uridine) and the trimethoxybenzene moiety instead of the ribose component. Therefore, the antibiotic molecules are only accumulated by *Ypt*UPh. The accumulation of trimethoprim by uridine phosphorylase results in a decrease in the effective concentration of the drug in bacteria of the genus *Yersinia*. This leads to a decrease in the number of antibiotic molecules that inhibit bacterial dihydrofolate reductase—the pharmacological target of this antibiotic [5, 6]. Therefore, the higher the level of expression of uridine phosphorylases in bacterial cells is, the larger the decrease in the efficiency of antibacterial therapy by the antibiotic trimethoprim is. Consequently, this antibiotic is less effective than the antibacterial drug against infectious diseases caused by bacteria of the genus *Yersinia*.

CONCLUSIONS

The three-dimensional structure of uridine phosphorylase from the bacterium *Yersinia pseudotuberculosis* was determined by X-ray crystallography and refined at an atomic resolution of 1.4 Å. The structure was deposited in the PDB (ID PDB: 4OF4). The spatial organization of this enzyme molecule was compared with that of uridine phosphorylases from the bacteria *Salmonella typhimurium* and *Escherichia coli* belonging to the same family as *Yersinia pseudotuberculosis*. There are only single amino-acid substitutions in these enzymes, whereas insertions and deletions are absent. In the enzymes under consideration, only insignificant changes in the positions of the side chains of different-type amino acids were found. Nevertheless, all these changes contribute to the stability of a particular secondary-structure element. The structural features of the buffering of the bacteriostatic drug trimethoprim by uridine phosphorylase were studied by molecular docking and classical molecular dynamics methods. These data will be helpful for optimizing antibacterial therapy using this drug. Differences in the binding of trimethoprim and the strong competitive uridine phosphorylase inhibitor 2,2'-anhydrouridine were found. These results extend the information necessary for the rational design of new antibacterial drugs for the treatment of not only pseudotuberculosis, but also of the bubonic plague and other diseases caused by bacteria of the family *Enterobacteriaceae*.

ACKNOWLEDGMENTS

This study was performed using the budgetary funding for the Shubnikov Institute of Crystallography of the Russian Academy of Sciences and was supported by the Russian Foundation for Basic Research (project no. 14-04-00952-a).

REFERENCES

1. C. Carnoy, N. Lemaitre, and M. Simonet, *The Comprehensive Sourcebook of Bacterial Protein Toxins* (Elsevier, Burlington, 2006).
2. R. Robins-Browne and E. Hartland, *Yersinia Species. InternationalHandbook of Foodborne Pathogens* (Marcel Dekker, New York, 2003).
3. J. F. MacFaddin, Biochemical Tests for Identification of Medical Bacteria (Williams & Wilkins, 1980).
4. M. B. Prentice, *Plague and Other Yersinia Infections. Harrison's Principles of Internal Medicine* (1950).
5. A. N. Kravchenko and B. N. Mishan'kin, Antibiot Khimioter. **37** (1), 17 (1992).
6. B. N. Mishan'kan, A. N. Kravchenko, and V. G. Maiskii, Z. Mikrobiol. Epidemiol. Immunobiol., No. 2, 24 (1989).
7. O. K. Molchan, N. A. Dmitrieva, D. V. Romanova, et al., Biochemistry (Mosc). **63** (2), 195 (1998).
8. M. Achtman, K. Zurth, G. Morelli, et al., Proc. Natl. Acad. Sci. USA **96** (24), 14043 (1999).
9. M. Zolotukhina, I. Ovcharova, S. Eremina, et al., Res. Microbiol. **154** (7), 510 (2003).
10. W. Kabsch, International Tables for Crystallography (Kluwer, Dordrecht, 2001).
11. P. R. Evans, Acta Crystallogr. D **67** (4), 282 (2011).
12. M. D. Winn, C. C. Ballard, K. D. Cowtan, et al., Acta Crystallogr. D **67** (4), 235 (2011).
13. A. J. McCoy, Acta Crystallogr. D **63** (1), 32 (2007).
14. P. D. Adams, P. V. Afonine, G. Bunkoczi, et al., Acta Crystallogr. D **66** (2), 213 (2010).
15. G. N. Murshudov, A. A. Vagin, and E. J. Dodson, Acta Crystallogr. D **53** (3), 240 (1997).
16. P. Emsley and K. Cowtan, Acta Crystallogr. D **60** (12), 2126 (2004).
17. P. Emsley, B. Lohkamp, W. G. Scott, et al., Acta Crystallogr. D **66** (4), 486 (2010).
18. I. W. Davis, A. Leaver-Fay, V. B. Chen, et al., Nucl. Acids Res. **35**, 375 (2007).
19. R. A. Friesner, J. L. Banks, R. B. Murphy, et al., J. Med. Chem. **47** (7), 1739 (2004).
20. T. A. Halgren, R. B. Murphy, R. A. Friesner, et al., J. Med. Chem. **47** (7), 1750 (2004).

21. D. Van Der Spoel, E. Lindahl, B. Hess, et al., J. Comput. Chem. **26** (16), 1701 (2005).

22. T. Schlesier and G. Diezemann, J. Phys. Chem. B **117** (6), 1862 (2013).

23. A. A. Lashkov, N. E. Zhukhlistova, A. G. Gabdulkhakov, et al., Crystallogr. Rep. **54** (2), 267 (2009).

24. M. V. Dontsova, A. G. Gabdoulkhakov, O. K. Molchan, et al., Acta Crystallogr. F **61** (4), 337 (2005).

25. T. T. Caradoc-Davies, S. M. Cutfield, I. L. Lamont, et al., J. Mol. Biol. **337** (2), 337 (2004).

26. S. T. Rao and M. G. Rossmann, J. Mol. Biol. **76** (2), 241 (1973).

27. A. A. Lashkov, N. E. Zhukhlistova, A. H. Gabdoulkhakov, et al., Acta Crystallogr. D **66** (1), 51 (2010).

28. W. L. DeLano, *The PyMOL Molecular Graphics System* (DeLano Scientific, San Carlos, CA, 2002).

Translated by T. Safonova